DOI: 10.1002/asia.200600260

Shape-Dependent Catalytic Activity of Silver Nanoparticles for the Oxidation of Styrene

Run Xu, Dingsheng Wang, Jiatao Zhang, and Yadong Li*[a]

Abstract: Metal nanoparticles with different shapes have different crystallographic faces. It is therefore of interest to study the effect of the shape of metal nanoparticles on their catalytic activity in various organic and inorganic reactions. Truncated triangular silver nanoplates with well-defined planes were synthesized by a simple solvothermal approach. The activity of these truncated triangular silver nanoparticles was compared with that of cubic and near-spherical silver nanoparticles in the oxidation of styrene in colloidal solution. It was found that the crystal faces of silver nanoparticles play an essential role in determining the catalytic oxidation properties. The silver nanocubes had the {100} crystal faces as the basal plane, whereas truncated triangular nanoplates and near-spherical nanoparticles predominantly exposed the most-stable {111} crystal faces. As a result, the rate of the reaction over the nanocubes was more than 14 times higher than that on nanoplates and four times higher than that on near-spherical nanoparticles.

Keywords: heterogeneous catalysis · nanostructures · oxidation · silver · X-ray diffraction

Introduction

Metal nanoparticles have been widely exploited for use in many different areas, such as photography,[1] catalysis,[2] biological labeling,[3] photonics,[4] optoelectronics,[5] information storage,[6] surface-enhanced Raman scattering,[7,8] and formulation of magnetic ferrofluids.[9] The intrinsic properties of a metal nanoparticle are mainly determined by its size, shape, composition, crystallinity, and structure.[10,11] In principle, one could control any one of these parameters to fine-tune the properties of these nanoparticles.[12,13]

The nanocatalysis field has undergone an explosive growth during the past decade. Most of the studies in the fields of nanocatalysis involve the use of spherical nanoparticles or nanoparticles of undetermined shapes. There are very few studies in which catalysis is conducted with nanoparticles of a specific shape in a colloidal solution. Narayanan and co-workers compared the stability and catalytic activity of tetrahedral, cubic, and spherical platinum nanoparticles in catalytic processes.[14,15] They found that the catalytic activity greatly depended on their shape, because different platinum nanoparticles have different fractions of atoms located at different corners and edges and different defects (resulting from the loss of atoms at these locations). Furthermore, nanoparticles of various shapes have specific faces. Choudary et al. reported that MgO hexagonal crystals exposing the most {100} planes were more active than nanocrystalline samples.[16] Campbell and co-workers reported that Cu particles with {110} planes were more active than those with {100} and {111} planes for the synthesis of methanol.[17] We recently reported that an easy solution-based hydrothermal method could be used to synthesize CeO_2 nanorods that expose mostly {001} and {110} planes and that the CeO_2 nanorods show higher catalytic activity than CeO_2 nanoparticles for CO oxidation.[18]

Silver catalysts have become increasingly important in the oxidation of olefins for the synthesis of industrially interesting products such as epoxides and aldehydes.[19–21] The face-centered cubic (fcc) structure of silver metal confers its tendency to nucleate and grow into nanoparticles with their surfaces bound by the lowest-energy {111} faces.[22] Most of the previous methods, in particular the wet chemical synthesis, were mainly confined to the preparation of nanowires, rods, spheres, disks, and plates.[23–26] Recently, silver nanocubes with less-stable {100} faces were synthesized by a polyol processes and attracted considerable interest owing to their structure.[10,27]

In the present study, we synthesized truncated triangular silver nanoparticles with well-defined planes by a simple sol-

[a] Dr. R. Xu, D. Wang, J. Zhang, Prof. Y. Li
Department of Chemistry
Tsinghua University
Beijing, 100084, (P. R. China)
Fax: (+86) 10-627-88-765
E-mail: ydli@mail.tsinghua.edu.cn

vothermal approach. Subsequently, we compared the activity of truncated triangular, cubic, and near spherical silver nanoparticles for the oxidation of styrene in a colloidal solution and we investigated the effect of crystal planes on the catalytic activity.

Results and Discussion

Preparation and Characterization of Truncated Triangular Silver Nanoplates

In our experiments, *N*,*N*-dimethylformamide (DMF) was used as solvent and reducing agent. Liz-Marzan and coworkers proposed the mechanism outlined in Equation (1):[28]

$$HCONMe_2 + 2Ag^+ + H_2O \longrightarrow 2Ag^0 + Me_2NCOOH + 2H^+ \quad (1)$$

The morphology and dimensions of the silver nanoplates were found to depend strongly on reaction conditions. Figure 1 shows the transmission electron microscopy (TEM) images of nanoplates synthesized under different conditions. When the concentration of $AgNO_3$ was 25 mM, truncated triangular silver nanoplates with an average edge length of (200±20) nm were obtained (Figure 1a). The initial concentration of $AgNO_3$ had to be lower than 50 mM, otherwise silver nanoplates of various sizes were obtained (Figure 1b and c). The reactions were also carried out at higher temperatures. However, nanoplates with different sizes and nanoparticles were observed (Figure 1d). PVP/$AgNO_3$ (PVP = poly(vinylpyrrolidone)) molar ratios between 1:1 and 3:1 favored the growth of triangular silver nanoplates. When the ratio was decreased, the silver nanoplates prepared had more round corners, and some particles had polyhedral structures. When the ratio was increased, small spherical or polyhedral silver crystals were the main products.

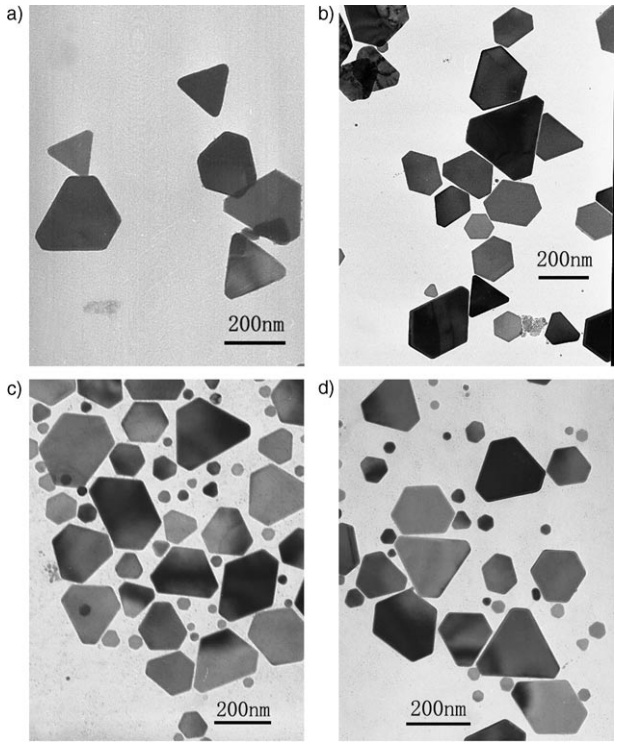

Figure 1. TEM images of truncated triangular silver nanoplates prepared under different synthesis conditions. a) 25 mM $AgNO_3$, 140 °C; b) 50 mM $AgNO_3$, 140 °C; c) 100 mM $AgNO_3$, 140 °C; d) 50 mM $AgNO_3$, 160 °C.

Structural Characterizations of Silver Nanoparticles

To investigate the effect of morphology on the properties of silver nanoparticles, near-spherical and cubic silver nanoparticles were synthesized by a polyol processes. The X-ray diffraction (XRD) patterns of the obtained silver nanoparticles are shown in Figure 2. The three peaks detected for the near-spherical silver nanoparticles were assigned to diffraction from the (111), (200) and (220) planes of face-centered cubic (fcc) silver, respectively. The lattice constant calculated from this pattern is 4.088 Å, a value in agreement with the literature report (α = 4.086 Å, JCPDS No. 04-0783). For the silver nanoplates, the overwhelmingly intensive peak located at 2θ = 38.02° corresponds to the diffraction of the (111) lattice plane of the fcc structure, whereas peaks arising from the other lattice planes were quite weak. This indicates that the (111) planes of silver nanoplates were highly orient-

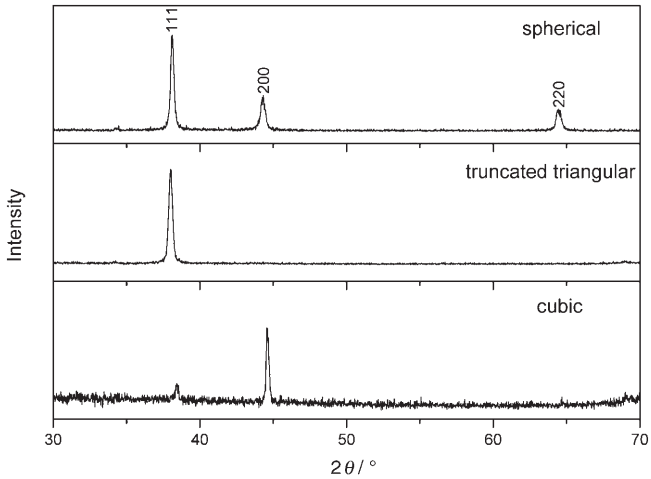

Figure 2. XRD patterns of the near-spherical, truncated triangular, and cubic silver nanoparticles.

Abstract in Chinese:
不同形貌的金属纳米颗粒由于其暴露的晶面不同从而会体现出不同的催化活性。本研究通过溶剂热合成的方法，得到了截角三角片、球型、立方体形状的Ag的纳米颗粒，并比较了它们对苯乙烯氧化的催化活性。研究发现立方体形状的Ag的纳米颗粒主要暴露的是高能态{100}晶面，而截角三角片和球型纳米颗粒主要暴露的是低能态{111}晶面。活性研究结果表明Ag纳米颗粒催化活性与其暴露晶面有关，高能晶面的催化活性较高。

ed, parallel to the supporting substrate. This structure feature is quite common for metal nanoplates, such as silver, gold, copper, and nickel plates.[22,29–31] Interestingly, the (200) diffraction peak showed the strongest intensity in the XRD pattern of silver nanocubes, and its intensity was nearly three times that of the commonly observed strongest (111) diffraction peak, whereas other peaks were not observed. It suggests that the product has a structure with a preferential [100] orientation. The unusual intensity of the (200) diffraction peak is a result of the strong tendency of the silver nanocubes to assemble into 2D arrays on the solid surface with the *c* axis perpendicular to the substrate upon the evaporation of the solvent.[27]

The morphology of the silver nanoparticles was further examined with TEM and scanning electron microscopy (SEM). Figure 3a is the TEM image of the obtained truncated triangular silver nanoplates. The SEM image demonstrates that the thickness of the nanoplates is about (15 ± 5) nm (upper-left inset). The upper-right inset shows an SAED (selected-area electron diffraction) pattern from the single nanoplate. The set of spots with the strongest intensity could be indexed to (220) reflections, which indicates that the nanoplates are single crystals with a {111} lattice plane as the basal plane. The inner set of spots should originate from the 1/3 (422) plane normally forbidden by an fcc lattice, which suggest that the faces parallel to the TEM grid are smooth and flat.[26] As shown in Figure 3b, the silver nanoparticles are really near spherical in shape with a mean diameter of (50 ± 10) nm. The SEM image indicated that the nanoparticles are not really spherical but have numerous faces (upper-left inset). The corresponding SAED pattern from the individual near-spherical nanoparticles with a [001] zone axis is shown in the upper right inset. These diffraction spots suggest that each nanoparticle is polycrystalline. The silver nanocubes are slightly truncated and have a mean edge length of (50 ± 5) nm with a smooth face (Figure 3c). They also have a strong tendency to assemble into 2D arrays with a regular checked pattern on the TEM grid (lower-left inset). The inset on the lower right shows an SAED pattern from one of square faces of the cube. The square symmetry of this pattern indicates that each silver nanocube is a single crystal bound mainly by six {100} planes.[10] Structural models of truncated triangular, near-spherical, and cubic silver nanoparticles are drawn in Figure 3d.

Catalytic Oxidation of Styrene over Truncated Triangular, Near-Spherical, and Cubic Silver Nanoparticles

The obtained silver nanoparticles were used as catalysts for the oxidation of styrene, and the reaction results are demonstrated in Table 1. Of all three catalysts, the silver nanocubes show the highest activity for the catalytic oxidation of styrene. The conversion of styrene over silver nanocubes is nearly three times higher than that on near-spherical nanoparticles under the same conditions. The conversion of styrene increased as the reaction time increased (Figure 4). In all cases benzaldehyde and styrene oxide were the main products. At the beginning of the reaction, the selectivity for styrene oxide was about 40%, while the selectivity for benzaldehyde continually increased with increasing reaction time. The formation of benzaldehyde from styrene can occur through two different routes. One possible pathway is the oxidation of the side chain, which causes breaking of the C=C bond to form benzalde-

Table 1. Summary of the catalytic performance and BET surface area for the truncated triangular, near spherical and cubic silver nanoparticles[a]

Nanoparticle shape	BET surface area [m^2g^-]	*t* [h]	Conv. [%]	B Sel. [%]	SO Sel. [%]
triangular	6.6	1	2	62	38
		3	13	68	32
		12	38	84	16
near spherical	3.2	1	4	60	40
		3	19	65	35
		12	45	79	21
cubic	3.7	1	10	56	44
		3	53	65	35
		12	82	81	19

[a] Conv. = conversion rate of styrene, B Sel. = selectivity for benzaldehyde, SO Sel. = selectivity for styrene oxide

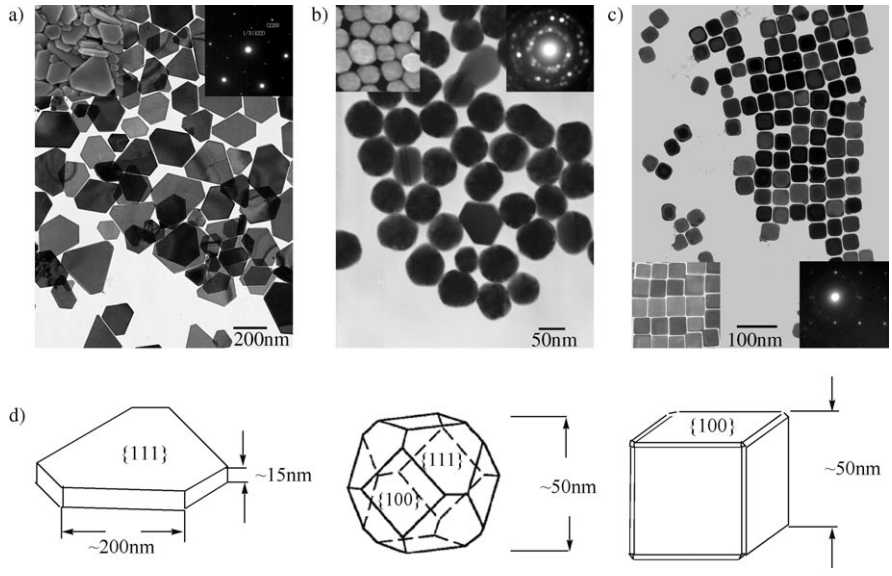

Figure 3. TEM image of a) truncated triangular nanoplates, b) near-spherical silver nanoparticles, and c) nanocubes, and d) their structural models. The insets show the scanning electron microscopy image (left) and the selected area electron diffraction pattern (right).

CHEMISTRY
AN ASIAN JOURNAL

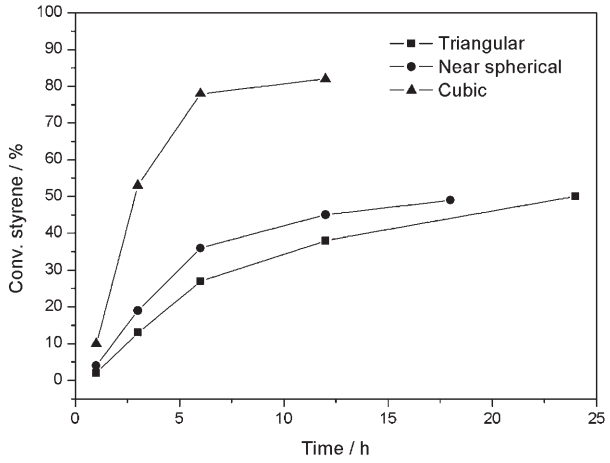

Figure 4. Catalytic performance of the silver nanoparticles in the oxidation of styrene with THBP (*tert*-butyl hydroperoxide).

hyde. Another way to form benzaldehyde from styrene is by epoxidation to form styrene oxide, which is then converted into benzaldehyde in the presence of peroxide. We believe the two different pathways may be occurring in parallel during the initial reaction stages. The selectivity for styrene oxide decreased with the further reaction owing to the enhanced reaction between styrene oxide and peroxide. As shown in Table 1, the selectivity over the three types of Ag nanoparticle was similar, which indicated that the shape possibly had little effect on the selectivity.

We consider that the effect of the shape of nanoparticles on the catalytic performance is likely determined by their surface area, the atoms on corners and edges, and the exposed crystal faces. Which factor is mainly responsible for catalytic performance? To answer the question, N_2-adsorption experiments were carried out with the different particles. The BET surface areas of the three types of nanoparticle are listed in Table 1. The BET surface area is highest for the truncated triangular nanoplates and lowest for near-spherical nanoparticles. The BET surface area of the nanocubes is close to that of the near-spherical nanoparticles. In general, if the surface area of the nanoparticles is the intrinsic property that determines the high catalytic activity, one would expect the truncated triangular silver nanoplates to be the most active and the near-spherical nanoparticles to be the least active, while the activity of the cubic nanoparticles would be inbetween. However, this is not consistent with our results.

Second, the near-spherical nanoparticles are formed with (111) and (100) faces with numerous edges and corners at the interface. We assume it to follow a truncated polyhedron structural model.[14,33] The slightly truncated cubic model is used for the silver nanocubes.[10] Based on the structural model, it could be roughly estimated that the fraction of atoms on edges and corners for near-spherical nanoparticles would be the highest and the fraction for truncated triangular nanoplates would be the lowest. If the atoms on the corners and edges (or defects resulting from them) are the dominantly active sites in catalysis, one would expect that the catalytic activity of the silver nanoparticles should decrease in the order near spherical > truncated cubic > truncated triangular. This is also not comparable with our results.

The different catalytic activities of the three types of silver nanoparticle cannot be explained by the different of surface area and the fraction of atoms on edges and corners, so the probably reason would be ascribed to their different crystal faces. As mentioned above, the near-spherical nanoparticles are composed of numerous {111} and {100} planes. The silver nanoplates predominantly exposed the well-defined and the most stable {111} planes, whereas in the silver nanocubes the less-stable {100} planes were predominantly exposed. As illustrated by Wang,[11] surface energies associated with different crystallographic planes are usually different, and a general sequence may hold, $\gamma(110) > \gamma(100) > \gamma(111)$. The planes with higher surface energy are more reactive.[10] Moreover, most catalytic reactions are sensitive to the surface structure of the catalysts, and it is well-known that the reactivity in structure-sensitive reactions depends on the crystal plane of the catalyst.[34] Previous computer simulations predicted that it is easier for adsorption and activation of ethylene and oxygen on crystal planes with higher surface energy.[35] On the basis of this result, the catalytic activity on the surface of the silver nanoparticles would decrease in the order $\gamma(110) > \gamma(100) > \gamma(111)$. That is the likely reason for the different catalytic activity on silver near-spherical nanoparticles, nanoplates, and nanocubes. To elucidate the remarkable effects of the catalyst shapes, the specific reaction rates (molecules of styrene converted over the surface area of silver nanoparticles) were calculated (Figure 5). It is noteworthy that the rate of conversion over nanocubes is over 14 times higher than that on nanoplates and four times higher than that on near-spherical nanoparticles. This result indicates that the catalytic activity on the {100} planes is higher than that on {111} planes, which is agreement with our conclusion.

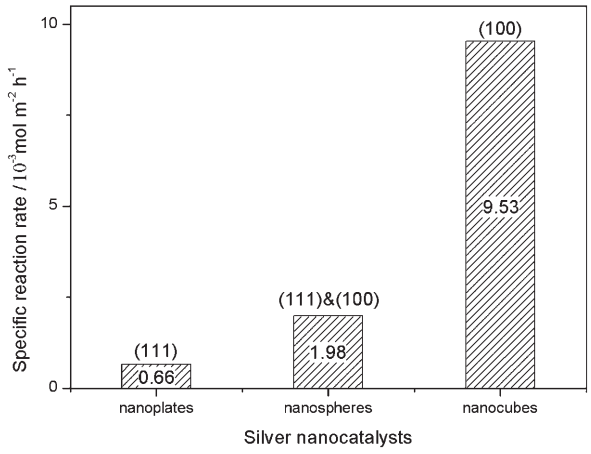

Figure 5. Specific reaction rate of styrene conversion over truncated triangular, near-spherical, and cubic silver nanoparticles. Reaction time: 3 h.

The three types of silver nanoparticles were prepared by different methods with PVP or cetyltrimethylammonium bromide (CTAB) as capping agents. It is possible that the different capping agents affect the surface chemistry of the nanoparticles. To understand the effect of the capping agent on the catalytic properties, a parallel reaction was carried out. We introduced trace amounts of CTAB into the colloid of Ag nanospheres. Some CTAB would adsorb on the surface of the Ag nanospheres. These particles were only slightly less catalytically active than the nanospheres without CTAB. This result indicates that at least the bromide does enhance the catalytic activity. On the other hand, both nanoplates and nanospheres were prepared with PVP as the capping agent; however, as the specific reaction rates over the nanospheres is three times higher than that over the nanoplates, it can be seen that the effect of the capping agent is limited in present work. The crystal faces of the silver nanoparticles play an essential role in determining the catalytic oxidation properties.

Conclusions

A simple and effective route has been developed for the preparation of silver nanoplate 2D structures. The obtained truncated triangular silver nanoplates were highly oriented single crystals with {111} planes as the basal planes. The morphology and dimensions of the silver nanoplates strongly depend on the concentration of $AgNO_3$, synthesis temperature, and the surfactant/$AgNO_3$ molar ratio. The cubic and near-spherical silver nanoparticles with well-defined planes were synthesized by polyol processes, and the activity of the truncated triangular, cubic, and near-spherical silver nanoparticles for the oxidation of styrene in colloidal solution were compared. The catalytic activity of the silver nanoparticles greatly depends on the crystal planes that the nanoparticles expose. The silver nanocubes show much higher styrene oxidation activity than near-spherical nanoparticles and nanoplates because of their more-reactive {100} planes. The present results suggest that a morphology-controlled synthesis method could result in an increase in more-reactive crystal planes and a decrease in less-reactive planes so as to optimize the catalytically active sites.

Experimental Section

In a typical synthesis of truncated triangular silver nanoplates, a solution of $AgNO_3$ in DMF (50 mM; 20 mL) was added dropwise to a solution of poly(vinylpyrrolidone) in DMF (50 mM; 20 mL). The mixture was then transferred to a 50-mL autoclave and heated at 140 °C under autogenetic pressure for 8 h. The final sample was obtained by centrifugation and washed with acetone and water. The near-spherical silver nanoparticles were synthesized by reducing $AgNO_3$ with N_2H_4 in the presence of PVP. An aqueous solution of $AgNO_3$ (50 mM; 20 mL) and N_2H_4 (75 mM; 20 mL) were added simultaneously to an aqueous solution of PVP (75 mM, MW = 30 000; 20 mL) at 25 °C under vigorous stirring. The silver nanocubes were synthesized by a CTAB-modified silver-mirror reaction according to a literature procedure.[26] The products were rinsed with ethanol several times to remove surfactants that remained on the surface of the final products.

Small drops of the each of the colloidal solutions were placed onto glass substrates and copper grids for XRD and TEM measurements, respectively. The XRD test was performed with a Bruker D8 Advance X-ray diffractometer with monochromated $Cu_{K\alpha}$ radiation ($\lambda = 1.5418$ Å). TEM and the corresponding SAED investigations were performed with a JEM-1200EX microscope operated at 120 kV. The SEM images of samples were obtained by using a JSM-6301F field-emission microscope. The BET surface areas of the catalysts were determined by N_2 adsorption at −196 °C on a Tristar 2010 Chemical Adsorption Instrument (Micrometritics).

The epoxidation of styrene over the silver nanoparticles was carried out at atmospheric pressure by treating the catalyst (50–100 mg) with styrene (10 mmol) and anhydrous TBHP (15 mmol) in a magnetically stirred glass reactor and heating at reflux for several hours. After the reaction mixture was cooled, the catalyst was separated from the reaction mixture by centrifugation. The reaction products were analyzed by GC/FID with an SE-30 column and N_2 as carrier gas. Some blank experiments were carried out. The conversion of styrene was below 1% in the absence of catalysts with TBHP as oxidant. No clear activity was detected when the TBHP was substituted with hydrogen peroxide or air.

Acknowledgements

This work was supported by the NSFC (90406003), the Foundation for Authors of National Excellent Doctoral Dissertations of the P. R. China, and the State Key Project of Fundamental Research for Nanomaterials and Nanostructures (2003CB716901).

[1] D. M. K. Lam, B. W. Rossiter, *Sci. Am.* **1991**, *265*, 48–53.
[2] L. N. Lewis, *Chem. Rev.* **1993**, *93*, 2693–2730.
[3] S. R. Nicewarner-Peña, R. G. Freeman, B. D. Reiss, L. He, D. J. Peña, I. D. Walton, R. Cromer, C. D. Keating, M. J. Natan, *Science* **2001**, *294*, 137–141.
[4] S. A. Maier, M. L. Brongersma, P. G. Kik, S. Meltzer, A. A. G. Requicha, H. A. Atwater, *Adv. Mater.* **2001**, *13*, 1501–1505.
[5] P. V. Kamat, *J. Phys. Chem. B* **2002**, *106*, 7729–7744.
[6] C. B. Murray, S. Sun, H. Doyle, T. Betley, *MRS Bull.* **2001**, *26*, 985–991.
[7] S. Nie, S. R. Emory, *Science* **1997**, *275*, 1102–1106.
[8] L. A. Dick, A. D. McFarland, C. L. Haynes, R. P. Van Duyne, *J. Phys. Chem. B* **2002**, *106*, 853–860.
[9] M.-P. Pileni, *Adv. Funct. Mater.* **2001**, *11*, 323–336.
[10] Y. Sun, Y. Xia, *Science* **2002**, *298*, 2176–2178.
[11] Z. L. Wang, *J. Phys. Chem. B* **2000**, *104*, 1153–1175.
[12] M. A. El-Sayed, *Acc. Chem. Res.* **2001**, *34*, 257–264.
[13] R. Xu, X. Wang, D. S. Wang, K. B. Zhou, Y. D. Li, *J. Catal.* **2006**, *237*, 426–430.
[14] R. Narayanan, M. A. El-Sayed, *Nano Lett.* **2004**, *4*, 1343–1348.
[15] R. Narayanan, M. A. El-Sayed, *J. Phys. Chem. B* **2005**, *109*, 12663–12676.
[16] B. M. Choudary, R. S. Mulukutla, K. J. Klabunde, *J. Am. Chem. Soc.* **2003**, *125*, 2020–2021.
[17] J. Yoshihara, C. T. Campbell, *J. Catal.* **1996**, *161*, 776–782.
[18] K. B. Zhou, X. Wang, X. M. Sun, Q. Peng, Y. D. Li, *J. Catal.* **2005**, *229*, 206–212.
[19] J. G. Allpress, J. V. Sanders, *Surf. Sci.* **1967**, *7*, 1–25.
[20] J. Q. Lu, M. F. Luo, H. Lei, X. H. Bao, C. Li, *J. Catal.* **2002**, *211*, 552–555.
[21] J. Q. Lu, M. F. Luo, H. Lei, C. Li, *Appl. Catal. A* **2002**, *237*, 11–19.
[22] R. J. Chimentao, I. Kirm, F. Medina, X. Rodriguez, Y. Cesteros, P. Salagre, J. E. Sueiras, *Chem. Commun.* **2004**, 846–847.
[23] Y. Sun, Y. Yin, B. Mayers, T. Herricks, Y. Xia, *Chem. Mater.* **2002**, *14*, 4736–4745.

[24] N. R. Jana, L. Gearheart, C. J. Murphy, *J. Phys. Chem. B* **2001**, *105*, 4065–4067.
[25] Y. Yin, Z. Li, Z. Zhong, B. Gates, Y. Xia, S. Venkateswaran, *J. Mater. Chem.* **2002**, *12*, 522–527.
[26] R. Jin, Y. Cao, C. A. Mirkin, K. L. Kelly, G. C. Schatz, J. G. Zheng, *Science* **2001**, *294*, 1901–1903.
[27] D. B. Yu, V. W. W. Yam, *J. Am. Chem. Soc.* **2004**, *126*, 13200–13201.
[28] I. Pastoriza-Santos, L. M. Liz-Marzan, *Langmuir* **1999**, *15*, 948–951.
[29] S. Chen, D. L. Carroll, *Nano Lett.* **2002**, *2*, 1003–1007.
[30] Y. Zhou, C. Y. Wang, Y. R. Zhu, Z. Y. Chen, *Chem. Mater.* **1999**, *11*, 2310–2312.
[31] A. C. Curtis, D. G. Duff, P. P. Edwards, D. A. Jefferson, B. F. G. Johnson, A. Kirkland, A. S. Wallace, *Angew. Chem.* **1988**, *100*, 1588–1590; *Angew. Chem. Int. Ed. Engl.* **1988**, *27*, 1530–1533.
[32] J. S. Bradley, B. Tesche, W. Busser, M. Maase, M. T. Reetz, *J. Am. Chem. Soc.* **2000**, *122*, 4631–4636.
[33] R. V. Hardeveld, F. Hartog, *Surf. Sci.* **1969**, *15*, 189–230.
[34] P. L. J. Gunter, J. W. Niemantsverdriet, F. H. Ribeiro, G. A. Somorjai, *Catal. Rev. Sci. Eng.* **1997**, *39*, 77–168.
[35] J. G. Serafin, A. C. Liu, S. R. Seyedmonir, *J. Mol. Catal. A* **1998**, *131*, 157–168.

Received: August 9, 2006
Published online: November 20, 2006

